Proc. Indian Acad. Sci. (*Chem. Sci.*), Vol. 115, No. 4, June 2003, pp 185–193

Lamellar multilayer hexadecylaniline-modified gold nanoparticle films deposited by the Langmuir–Blodgett technique

ANITA SWAMI, ASHAVANI KUMAR and MURALI SASTRY*
Materials Chemistry Division, National Chemical Laboratory, Pune 411 008, India
e-mail: sastry@ems.ncl.res.in

MS received 30 October 2002; revised 22 March 2003

Abstract. Organization of hexadecylaniline (HDA)-modified colloidal gold particles at the air–water interface and the formation thereafter of lamellar, multilayer films of gold nanoparticles by the Langmuir–Blodgett technique is described in this paper. Formation of HDA-capped gold nanoparticles is accomplished by a simple biphasic mixture experiment wherein the molecule hexadecylaniline present in the organic phase leads to electrostatic complexation and reduction of aqueous chloroaurate ions, capping of the gold nanoparticles thus formed and phase transfer of the now hydrophobic particles into the organic phase. Organization of gold nanoparticles at the air–water interface is followed by surface pressure–area isotherm measurements while the formation of multilayer films of the nanoparticles by the Langmuir–Blodgett technique is monitored by quartz crystal microgravimetry, UV-Vis spectroscopy, Fourier transform infrared spectroscopy and transmission electron microscopy.

Keywords. Lamellar multilayer films; hexadecylaniline-modified gold nanoparticle films; Langmuir–Blodgett technique.

1. Introduction

There is growing interest in the organization of nanoparticles in two- and three-dimensional superstructures. The main challenge in this area is to develop protocols for the organization of crystalline arrays of nanoparticles wherein both the size and separation between the nanoparticles in the arrays can be tailored. Applications based on the collective properties of the organized particles require flexibility in controlling the nanoarchitecture of the film.[1] Attempts have been made to assemble nanoparticles in two-dimensional structures by a variety of methods that include self-assembly of the particles during solvent evaporation,[2] immobilization by covalent attachment at the surface of the self-assembled monolayers[3,4] or surface modified polymers,[5] electrophoretic assembly onto suitable substrates,[6] electrostatic attachment to Langmuir monolayers at the air–water interface[7–11] and air–organic solvent interface,[12] and by diffusion into ionizable fatty lipid films.[13–15]

*For correspondence

The degree of control over molecular level organization of amphiphiles and ions that may be exercised at the air–water interface has resulted in its extensive use in the organization of large inorganic ions[16–18] and biological macromolecules.[19–22] In this laboratory, negatively charged carboxylate ion-derivatized colloidal silver,[7,10] gold[8,11] and Q-state CdS[9] nanoparticles have been electrostatically co-ordinated to charged Langmuir monolayers and transferred onto solid substrates by the Langmuir–Blodgett (LB) technique. Fendler and co-workers first demonstrated that surface modified hydrophobic nanoparticles may also be organized at the air–water interface and that multilayer films of the nanoparticles could be formed on suitable substrates by the LB technique.[23] A number of other groups have now used this method to form multilayer films of gold nanoparticles,[24–28] polymer-capped platinum colloidal particles[29] and buckyballs.[30] Insofar as gold nanoparticles are concerned, the key step consists of surface modification of the particles to render them hydrophobic and amenable to organization on the surface of water. The Brust synthesis procedure,[31] wherein gold nanoparticles are synthesized and capped with alkanethiols in a non-polar organic phase, continues to be the most popular means of obtaining hydrophobic gold nanoparticles that are readily dispersible in different non-polar/weakly polar organic solvents.[24] An alternative method for obtaining hydrophobic gold nanoparticles synthesized in water by electrostatic coupling with fatty amine molecules present in non-polar organic solvents has been demonstrated in this laboratory.[32]

Recently, some of us have developed a considerably simplified single-step alternative to the Brust method for the synthesis of hydrophobized gold nanoparticles.[33] This process essentially consists of vigorous stirring of a biphasic mixture of aqueous chloroauric acid solution and a non-polar organic phase containing the multifunctional molecule, 4-hexadecylaniline (HDA).[33] During the stirring process, electrostatic complexation of the HDA molecules with $AuCl_4^-$ ions is followed by spontaneous reduction of chloroaurate ions by HDA. The HDA molecules also bind to the gold nanoparticles thus formed thereby rendering them hydrophobic and soluble in the organic phase.[33] It would be of interest to study the assembly of hydrophobic HDA-capped gold nanoparticles synthesized as briefly described above on the surface of water and study the Langmuir–Blodgett (LB) film forming capability of the gold nanoparticle monolayers on different substrates. It is these issues that we address in this paper, the details of which are presented below.

2. Experimental details

In a typical experiment, 50 ml of 10^{-3} M aqueous solution of $HAuCl_4$ was taken in a beaker along with 50 ml solution of 10^{-3} M HDA in chloroform. The biphasic mixture was stirred vigorously on a magnetic stirrer for 1 h following which the appearance of reddish colour in the organic phase could be discerned. The appearance of colour in the organic phase clearly indicates formation of nanoparticles in that medium. Thereafter the organic layer was separated out and rotovapped to yield a powder of hydrophobized gold nanoparticles as described elsewhere.[33] This powder was purified by washing 4–5 times with acetonitrile to remove uncoordinated HDA molecules in the organic solution and dried in nitrogen atmosphere. The HDA-capped gold nanoparticle powder could be readily dispersed in different organic solvents such as toluene, benzene, hexane, chloroform etc.

100 μl of hydrophobized HDA-capped gold particle solution in chloroform (concentration 8 mg/ml) was spread on the surface of double-distilled water at pH 6·5 in a

model 611 Nima LB trough. Pressure–area (π–A) isotherms of this solution were recorded at room temperature at a compression and expansion rate of 100 cm^2/min. A standard Wilhelmy plate was used for surface pressure sensing. Multilayer films of the colloidal particles of different thickness were formed by the versatile LB technique[16] at a surface pressure of 15 mN/m and a deposition rate of 20 mm/min with a waiting time of 1 min between dips. LB films of the HDA-capped gold nanoparticles were deposited on quartz slides, Si (111) wafers, gold-coated AT-cut quartz crystals and carbon-coated transmission electron microscopy (TEM) grids for UV-Vis spectroscopy, Fourier transform infrared spectroscopy (FTIR), quartz crystal microbalance (QCM) and electron microscopy measurements respectively. The quartz and Si (111) substrates were hydrophobized by depositing 3 monolayers of lead arachidate prior to transfer of the gold nanoparticle monolayers. It is known that metal salts of fatty acids (cadmium arachidate, lead arachidate etc.) form stable monolayers strongly bound to Si substrates and consequently, this strategy was used to hydrophobize the Si (111) wafers. The hydrophobization of the support resulted in significantly better transfer ratios of the nanoparticle monolayers. For the LB films grown on different substrates, monolayer transfer was observed both during the upward and downward strokes of the substrate at close to unity transfer ratio. Contact angle measurements of a sessile water drop (1 μl) were also carried out on the gold colloidal particle multilayer films deposited on quartz substrates using a Rame Hart 100 goniometer. The frequency counter used for the QCM studies was an Edward FTM5 instrument operating at a frequency stability and resolution of ± 1 Hz. For the 6 MHz crystal used in this investigation, this translates into a mass resolution of 12 ng/cm^2. FTIR measurements of the gold colloidal particle LB films were carried out in the diffuse reflectance mode at a resolution of 4 cm^{-1} on a Perkin–Elmer Instruments Spectrum-1 FT-IR spectrometer. UV-Vis spectroscopy measurements of all the samples were performed on a Hewlett–Packard HP 8542A diode array spectrophotometer operated at a resolution of 2 nm. TEM measurements of the gold nanoparticle films formed at the air-water interface and transferred onto a carbon-coated copper grid were carried out on a JEOL model 1200EX instrument operated at an accelerating voltage of 120 kV.

3. Results and discussion

The assembly of HDA-capped gold nanoparticles into monolayers on the surface of water was followed by π–*A* isotherm measurements. Figure 1a shows the π–*A* isotherm recorded from the Langmuir monolayer of the HDA-capped gold nanoparticles 15 min after spreading the monolayer. The arrows in the isotherms indicate the compression and expansion cycles of the monolayer. It is observed that during compression, the surface pressure builds up to reach a limiting value of ~18 mN/m. Further compression resulted a drastic fall in the surface pressure indicating collapse of the HDA-capped gold nanoparticle monolayer. From the π–*A* isotherm measurements (figure 1a), a region of reasonably large incompressibility is seen to occur up to surface pressure of $\approx$ 15 mN/m and therefore, multilayer films of HDA-capped gold nanoparticles of different thickness were transferred onto different substrates at this surface pressure by the LB technique for further studies (figure 1b). During expansion of the monolayer, some hysteresis is observed, but this is not surprising given that the gold nanoparticles cannot be considered to be truly amphiphilic. The hysteresis observed may also arise due to rearrangement of the gold nanoparticles within domains (and reorganization of the domains themselves) on

release of surface pressure with a time-scale larger than the experimentally controlled expansion rate of the monolayer.

The mass uptake during successive immersion cycles of an AT-cut quartz crystal in the HDA-capped gold nanoparticle monolayer was studied using QCM and the data obtained are shown in figure 2a. It can be seen from the QCM data that the mass uptake during successive immersion cycles is quite constant and independent of the substrate immersion cycle. This indicates that the gold nanoparticle monolayer is transferred onto the substrate without a significant variation in nanoparticle density up to fairly large thickness of the built-up LB films. The solid line is a nonlinear least squares fit to the QCM data and yields a mass uptake/bilayer (corresponding to one immersion cycle of the quartz crystal in the water subphase) of 1198 ng/cm^2. As mentioned in the experimental section, close to unity transfer ratios were observed both during the compression and expansion cycles clearly indicating transfer of bilayers of the gold nanoparticles during each immersion cycle. Thus, the QCM measurements show that the HDA-capped gold nanoparticle monolayers are transferred in a layer-by-layer fashion by the LB technique without significant variation in the nanoparticle packing density in the different layers.

Contact angles of a sessile water drop on LB films of the HDA-capped Au nanoparticles of different thickness viz. 6 monolayers (MLs), 10 ML, 16 ML and 20 ML transferred to hydrophobized quartz substrates were measured and are shown in figure 2b. It is observed that the contact angle (averaged over 4 different readings over the film surface) is almost identically 99^o in all cases and is clearly independent of the thickness of the film. The contact angle of the underlying quartz substrate was measured to be 55°. In an earlier study of gold nanoparticles rendered hydrophobic by electrostatic complexation of octadecylamine molecules with nanoparticle surface-bound carboxylic acid functional groups, it was observed that the contact angles for LB films of the nanoparticles increased steadily with thickness from 67° (4 ML) to 87° (18 ML).[34] The fact that the LB films of the HDA-capped gold nanoparticles are extremely hydrophobic

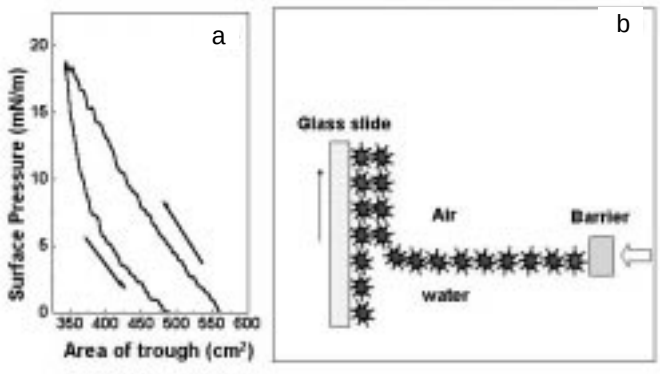

Figure 1. (**a**) π–A isotherm recorded during one compression and expansion cycle of HDA-capped gold nanoparticles 15 min after spreading the nanoparticle monolayer on water. The arrows indicate the compression and expansion regions in the isotherm. (**b**) Schematic showing the layer-by-layer deposition of HDA-capped gold nanoparticle monolayers from the surface of water.

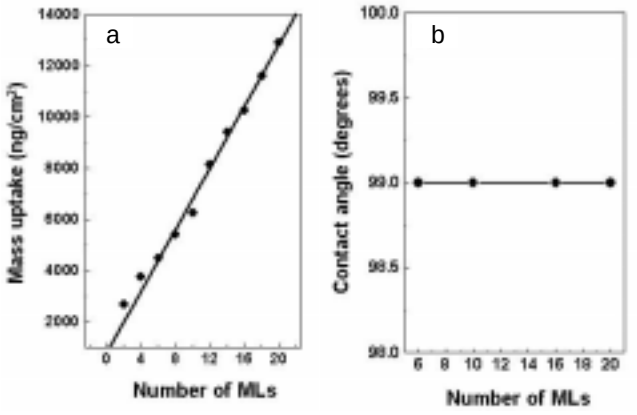

Figure 2. (**a**) QCM mass uptake data plotted as a function of number of monolayers of the HDA-capped gold nanoparticles transferred onto the QCM crystal by the LB technique. The solid line is a nonlinear least squares fit to the QCM data. (**b**) Contact angle measurements of a sessile water drop on HDA-capped gold nanoparticle LB films plotted as a function of thickness (in terms of number of monolayers transferred) of the film. The solid line is to aid the eye and has no physical significance.

even for small thicknesses of the films indicates that the HDA molecules form close packed monolayers on the surface of the gold nanoparticles. This result also indicates that the HDA-capped gold nanoparticles transferred from the surface of water are themselves packed into a highly close-packed assembly within the Langmuir monolayers. Our observation of extremely uniform nanoparticle bilayer transfer characteristic of classical amphiphiles during LB film formation (QCM measurements, figure 2a) is therefore surprising. We believe this may be due to facile interdigitation of hydrocarbon chains of the gold nanoparticle surface-bound HDA molecules with underlying gold nanoparticle monolayers during film growth in a sort of 'zipper' action as illustrated in figure 1b.

Figure 3a shows the optical absorption spectra recorded as a function of number of monolayers of HDA-capped gold nanoparticles transferred from the surface of water onto hydrophobized quartz substrates. The inset of the figure shows pictures of the films whose spectra are displayed in the main part of the figure. We observe a monotonic increase in the intensity of a strong and broad resonance, which occurs at approximately 540 nm, with number of monolayers transferred (number of monolayers in the LB film is given next to the respective spectra). This absorption band is due to excitation of surface plasmon vibrations in the gold nanoparticles present in the LB films and gives the particles their characteristic pink/purple colour.[15] The wavelength at which resonance occurs (540 nm) is considerably red-shifted with respect to the absorption band for aqueous colloidal gold solutions where it occurs in the range 510–525 nm. The shift observed in the LB films of gold nanoparticles reflects a variation in the dielectric properties of the medium in which the gold nanoparticles are embedded and clearly shows fairly dense packing of the gold nanoparticles.[16,34] The pictures of the LB films of gold nanoparticles (inset, figure 3a) illustrates beautifully the increase in intensity of purple colour in the LB films as the number of nanoparticle layers is increased. Figure 3b shows a plot of the intensity of absorption at 540 nm as a function of the number of layers

in the LB films for which the spectra are shown in figure 3a. A linear increase in the absorbance with number of monolayers of HDA-capped gold nanoparticles in the LB films is seen indicating that excellent layer-by-layer transfer of the hydrophobized gold nanoparticles had occurred. This result, together with QCM results presented in figure 2a, clearly shows that multilayer LB films of the gold nanoparticle monolayer organized at the air-water interface may be grown without a significant change in the cluster density in the different layers.

The FTIR spectrum of a 20 ML gold nanoparticle LB film grown on a hydrophobized Si (111) wafer was recorded and the spectrum obtained in the regions 3400–2600 cm^{-1} and 1600–1300 cm^{-1} is plotted in figures 4a and b respectively. The methylene anti-symmetric and symmetric vibration modes at 2920 and 2850 cm^{-1} respectively are clearly seen in figure 4a. We would like to mention here that the features at 2920 and 2850 cm^{-1} observed in the FTIR spectrum of a film of just 3 monolayers of lead arachidate deposited on Si (111) wafer were extremely weak (data not shown). Consequently, the 2920 and 2850 cm^{-1} resonances observed in the 20 ML LB film of the gold nanoparticles deposited on the extremely thin lead arachidate base arise from the hydrocarbon chains in the HDA molecules surrounding the gold nanoparticles. The position of the antisymmetric and symmetric vibrations of methylene groups of HDA molecules present on the surface of gold nanoparticles indicates clearly that the hydrocarbon chains capping the gold nanoparticles are closely packed without a significant density of defects in the chains.[35] The $-NH_2$ antisymmetric vibrational mode, which normally occurs at 3300 cm^{-1} for free alkylamines,[15,34] is absent in the LB films of HDA-capped gold indicating good complexation of the surface-bound HDA molecules with the gold surface. In the lower spectral region (figure 4b), the feature at 1460 cm^{-1} arises due to methylene scissoring

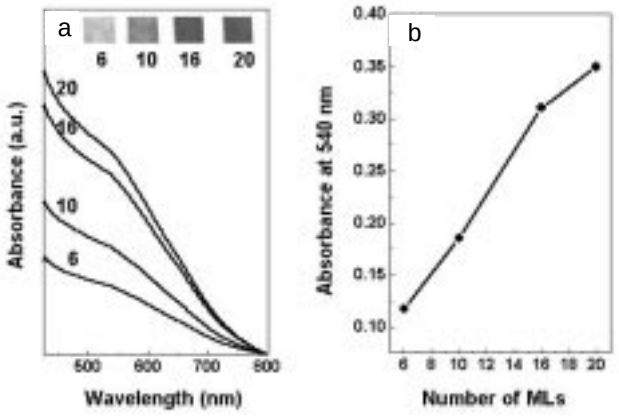

Figure 3. (**a**) UV-Vis spectra recorded from HDA-capped gold nanoparticle LB films of different thickness transferred onto hydrophobized quartz substrates. The number of monolayers of the gold nanoparticles in the LB films is indicated next to the respective curve. The inset shows pictures of the gold nanoparticle LB films on quartz (thickness indicated next to the films). (**b**) A plot of intensity of the surface plasmon resonance (absorbance at 540 nm) plotted as a function of number of mono-layers of HDA-capped gold nanoparticles in LB films grown on quartz.

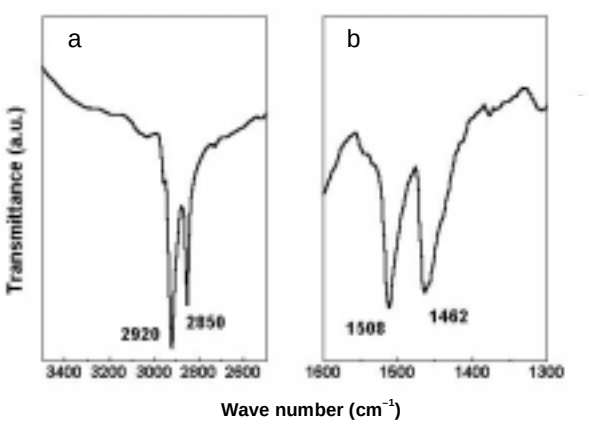

Figure 4. FTIR spectra recorded from a 20-ML HDA-capped gold nanoparticle LB film on a Si (111) wafer in two different spectral windows: (**a**) 3400–2600 cm^{-1} and (**b**) 1600–1300 cm^{-1}.

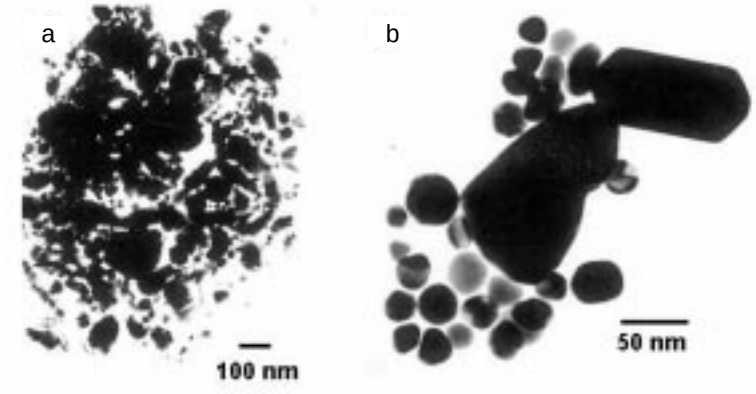

Figure 5. TEM images at low (**a**) and high magnification (**b**) of one monolayer of HDA-capped gold nanoparticles transferred onto a carbon-coated TEM grid by vertical lifting.

modes of vibration, the splitting of which is known to be a sensitive indicator of the crystalline packing of hydrocarbon chains.[36] The fact that this feature is broad without discernible splitting indicates that the chains, though close packed are not in a crystalline environment. This is likely to be a consequence of the surface curvature of the gold nanoparticles. Another feature at 1508 cm^{-1} is observed which is assigned to the N–H bending vibration mode arising from the HDA molecules bound to the gold nanoparticle surface.

Figures 5a and b show representative TEM images at different magnifications recorded from one monolayer of HDA-capped gold nanoparticles transferred by the LB method

onto a carbon-coated TEM grid. At low magnification, a dense assembly of irregularly shaped gold nanoparticles is observed. The dense packing within domains is consistent with the contact angle measurements that indicate very hydrophobic monolayers of the gold nanoparticles (figure 2b). Both images reveal highly polydisperse particles of different shapes, the particle sizes ranging from 20–100 nm. At higher magnification (figure 5b), the morphology of the individual gold nanoparticles is observed in greater detail. In this assembly, polyhedral gold nanoparticles are seen together with prismatic and rod-shaped gold nanoparticles. The reasons for the morphology exhibited by the gold nanoparticles is not clear at this stage.

In conclusion, it has been demonstrated that hydrophobic gold nanoparticles synthesized by the spontaneous reduction of aqueous chloroaurate ions by 4-hexadecylaniline molecules may be organized on the surface of water to yield close-packed nanoparticle Langmuir monolayers. Good quality multilayer LB films of the gold nanoparticles can be grown on different substrates in a lamellar fashion without significant variation in the nanoparticle density in the individual layers.

Acknowledgements

AS and AK would like to thank the Council for Scientific and Industrial Research (CSIR), New Delhi, for research fellowships. This work was funded by a grant to MS from the Department of Science and Technology, Govt. of India and is gratefully acknowledged. The authors thank Ms Renu Pasricha, for assistance with TEM measurements.

References

1. Collier C P, Saykally R J, Shiang J J, Henriches S E and Heath J R 1997 *Science* **277** 1978
2. Wang Z L 1998 *Adv. Mater.* **10** 13
3. Colvin V L, Goldstein A N and Alivisatos A P 1992 *J. Am. Chem. Soc.* **114** 522
4. Gole A, Sainkar S R and Sastry M 2000 *Chem. Mater.* **12** 1234
5. Freeman F G, Grabar K C, Allison K J, Bright R M, Davis G A, Guthrrie A P, Hommer M B, Jackson M A, Smith P C, Walter D G and Natan M J 1995 *Science* **267** 1629
6. Giersig M and Mulvaney P 1993 *J. Phys. Chem.* **97** 6334
7. Sastry M, Mayya K S, Patil V, Paranjape D V and Hegde S G 1997 *J. Phys. Chem.* **B101** 4954
8. Patil V, Mayya K S, Pradhan S D and Sastry M 1997 *J. Am. Chem. Soc.* **119** 9281
9. Mayya K S and Sastry M 1998 *Langmuir* **14** 74
10. Sastry M, Mayya K S and Patil V 1998 *Langmuir* **14** 5921
11. Sastry M, Rao M and Ganesh K N 2002 *Acc. Chem. Res.* **35** 847
12. Mayya K S and Sastry M 1999 *Langmuir* **15** 1902
13. Sastry M, Patil V and Mayya K S 1997 *Langmuir* **13** 4490
14. Sastry M, Patil V and Sainkar S R 1998 *J. Phys. Chem.* **B102** 1404
15. Patil V, Malvankar R B and Sastry M 1999 *Langmuir* **15** 8197, and references therein
16. Ulman A 1991 *An introduction to ultrathin organic films: From Langmuir–Blodgett to self assembly* (San Diego, CA: Academic Press)
17. Ganguly P, Paranjape D V and Sastry M 1993 *J. Am. Chem. Soc.* **115** 793
18. Clemente-Leon M, Agricole B M, Mingotaud C, Gomez-Garcia C J, Coronado E and Delhaes P 1997 *Langmuir* **13** 2340
19. Reiter R, Motschmann M and Knoll W 1993 *Langmuir* **9** 2430
20. Riccio A, Lanzi M, Antolini F, De Nitti C, Tavani C and Nicolini C 1996 *Langmuir* **12** 1545
21. Nakamura F, Ijiro K and Shimomura M 1998 *Thin Solid Films* **327** 603

22. Ramakrishnan V, D'Costa M, Ganesh K N and Sastry M 2002 *Langmuir* **18** 6307
23. Fendler J H and Meldum F 1995 *Adv. Mater.* **7** 607, and references therein
24. Heath J R, Knobler C M and Leff D V 1997 *J. Phys. Chem.* **B101** 189
25. Chi L F, Rakers S, Hartig M, Fuchs H and Schmid G 1998 *Thin Solid Films* **327–329** 520
26. Bourgoin J F, Kergueris C, Lefevre E and Palacin S 1998 *Thin Solid Films* **327–329** 515
27. Li W, Xu R, Wang L, Cui H and Xi S 1999 *Mol. Cryst. Liq. Cryst.* **A337** 185
28. Burghard M, Philipp G, Roth S, Von Klitzing K, Pugin R and Schmid G 1998 *Adv. Mater.* **10** 842
29. Sastry M, Patil V, Mayya K S, Paranjape D V, Singh P and Sainkar S R 1998 *Thin Solid Films* **324** 239
30. Ganguly P, Paranjape D V, Patil K R, Chaudhari S K and Kshirsagar S T 1992 *Indian J. Chem.* **A31** F42
31. Brust M, Walker M, Bethell D, Schiffrin D J and Whyman R 1994 *J. Chem. Soc., Chem. Commun.* 801
32. Sastry M, Kumar A and Mukherjee P 2001 *Colloid. Surf.* **A181** 255
33. Selvakannan P R, Mandal S, Pasricha R, Adyanthaya S D and Sastry M 2002 *Chem. Commun.* 1334
34. Sastry M, Gole A and Patil V 2001 *Thin Solid Films* **384** 125
35. Hostetler M J, Stokes J J and Murray R W 1996 *Langmuir* **12** 3604
36. von Sydow R G 1961 *J. Mol. Spectrosc.* **7** 116